Contemporary Mathematics
https://ojs.wiserpub.com/index.php/CM/

Research Article

Distributed Iterative Learning Impedance Control for a Team of Robot Manipulators with Varying Trial Lengths

Wenli Zhang, Dongdong Yue, Chuang Chen, Jiantao Shi*

College of Electrical Engineering and Control Science, Nanjing Tech University, Nanjing, 211816, China
E-mail: sjt11@tsinghua.org.cn

Received: 21 May 2025; **Revised:** 13 June 2025; **Accepted:** 16 June 2025

Abstract: This article presents a distributed iterative learning impedance control algorithm for a team of robot manipulators with varying trial lengths. This approach enables each manipulator to achieve the desired impedance model only using the impedance information of its neighbors, eliminating the need for direct access to the desired joint angle profiles. Furthermore, the proposed scheme addresses the challenge of randomly varying operation lengths across iterations. This capability is particularly important for ensuring the robustness of practical industrial systems, where trial durations vary due to dynamic task requirements. It is demonstrated that the impedance error L^2-norm of each manipulator converges to zero as the iteration index approaches infinity even under variable-length operations. Finally, experimental validation using collaborative robot manipulators confirms the effectiveness, adaptability, and practicality of the proposed method.

***Keywords*:** distributed iterative learning, impedance control, robot manipulators, varying trial lengths

MSC: 93C85, 93A14, 93B35, 93C55, 68T40

1. Introduction

Iterative Learning Control (ILC) was developed to enable machinery to improve performance through human-inspired, cycle-based learning from repeated tasks. As an innovative control method for repetitive industrial processes with fixed operation intervals and consistent learning objectives [1–3], ILC leverages past control experiences to enhance current system performance. It requires only knowledge of the boundary of the system gradient rather than an exact system model, offering an efficient solution to handle uncertainties. In recent years, robot manipulators have become an important application area for ILC.

In practical operations, due to the limitations of a single manipulator's load capacity and working range, multiple manipulators often need to collaborate, such as when transporting large objects on construction sites in manufacturing factories. Similarly, for paralyzed patients, using multiple manipulators to simultaneously train both arms and legs can more effectively help them learn to coordinate different parts of their body. This is generally achieved through the implementation of cooperative impedance control techniques [4–10]. Despite significant progress in impedance control and ILC, most existing studies rely on centralized architectures that assume full access to joint angle trajectories.

DOI: https://doi.org/10.37256/cm.6420257284

However, in practical multi-robot systems, such assumptions are often unrealistic due to communication constraints, partial observability, or decentralized task execution. For instance, when a group of manipulators collaboratively lifts a heavy object, only one manipulator may know the destination, and the others need to coordinate through interactions with their neighbors. For such cases, a distributed impedance control framework is more practical, as it allows each manipulator to coordinate using only local information and relative configurations with its neighbors.

Building upon the principles of impedance control, recent studies have strategically integrated Iterative Learning Control (ILC) into robotic and Multi-Agent Systems (MASs) to enhance performance in dynamic tasks. In [11], an iterative learning framework achieves finite-time consensus for second-order leader-follower MASs, ensuring precise coordination under time-critical constraints. Extending these principles, [12] proposes an adaptive neural-Fourier ILC scheme that enables robust consensus and formation control for nonlinear MASs, effectively suppressing control chattering under disturbances through hybrid approximation strategies. Further addressing cybersecurity challenges in networked environments, [13] develops a dual-domain triggered ILC architecture for switched systems under Denial-of-Service (DoS) attacks, combining real-time attack detection, buffer compensation, and Lyapunov-based stability guarantees to maintain bounded tracking errors while minimizing network traffic. Together, these advancements demonstrate how the synergistic integration of impedance control and ILC fosters adaptability, precision, and resilience in multi-robot systems operating within dynamic, uncertain, and adversarial environments.

In robot-assisted applications, a combined impedance control and sliding mode ILC approach was developed to manage unknown model parameters and human-robot interaction disturbances in bathing tasks [14], while a gravity compensation ILC scheme with steady-state scaling was proposed for trajectory tracking in arthroscopic surgery under dynamic uncertainties [15]. Moreover, [16] proposed a formation-based decentralized Iterative Learning Cooperative Impedance Control (ILCIC) architecture to enable manipulators to achieve desired impedance models under iteration-varying tasks, even without direct access to desired angle trajectories. Collectively, these studies highlight the effectiveness of ILC and impedance control in addressing learning and control challenges in dynamic and uncertain collaborative environments.

ILC inherently requires a constant operation length per iteration to achieve convergent learning of control/system information. Yet real-world uncertainties frequently disrupt this condition. In bipedal robot applications, for instance, gaits consist of temporally variable phases, inherently conflicting with the constant-duration assumption [17]. Another example is seen in the analysis of laboratory-scale gantry cranes, where ILC is applied to trajectory tracking tasks, but iterations terminate prematurely when the output exceeds specified boundaries, leading to variable trial lengths [18]. Furthermore, in studies on Functional Electrical Stimulation (FES) for drop foot treatment, trials may need to be stopped early for safety reasons, resulting in variable trial durations [19]. These real-world examples highlight the need to address the issue of variable trial lengths in the design and analysis of ILC. By introducing control algorithms that accommodate variable-length operations, the applicability of ILC in dynamic and complex environments can be significantly expanded.

In recent years, several ILC methods have been developed to handle the issue of varying trial lengths. Li et al. [20–22] introduced a stochastic model based on Bernoulli variable distributions and iterative averaging operators to address information loss caused by prematurely terminated trials. Shen et al. [23, 24] later proposed an analytical method independent of averaging operators, demonstrating the strong convergence of p-type ILC under variable operation lengths. Furthermore, [25] proposed an ILC scheme for stochastic time-varying systems with variable pass lengths, ensuring bounded tracking errors through a modified iteration-average operator. Recent advances extend these results to nonlinear systems, such as adaptive control for Multiple-Input Multiple-Output (MIMO) nonlinear systems achieving rapid error convergence under nonuniform trial lengths [26], segmented compensation methods for discrete time-varying systems with varying initial conditions [27], and learning schemes with forgetting factors for impulsive nonlinear systems, ensuring convergence and robustness [28]. These studies collectively provide robust tools to address the challenge of variable trial lengths.

However, the aforementioned works primarily focus on systems represented by mathematical models and investigate only centralized methods. To date, Distributed Iterative Learning Impedance Control (DILIC) for multi-manipulator systems operating with varying-length trials remains unexplored. This gap directly motivates our work. Our core contributions are:

(i) Distributed Framework for Varying-Trial-Length Impedance Control: Compared to centralized variable-trial-length ILC methods (e.g., [21, 24]), this work proposes a global-trajectory-free distributed architecture, significantly reducing communication load and resolving partial observability bottlenecks in practical collaboration.

(ii) Adaptive Learning Mechanism for Physical Uncertainties: Unlike model-dependent strategies (e.g., [26, 28]), our approach compensates for unmodeled dynamics (e.g., joint friction) through online adaptive learning, substantially enhancing adaptability in dynamic environments.

(iii) Hardware Validation of Engineering Feasibility: Addressing the limitation of existing studies remaining simulation-only (e.g., [20, 25]), we implement hardware validation of varying-trial-length ILC on a multi-manipulator platform, successfully handling real-world disturbances (e.g., emergency stops) and bridging the theory-to-practice gap in distributed learning control.

This work unfolds through six cohesive sections: Section II establishes the graph-theoretic foundation and formalizes the impedance control problem. Building on this, Section III develops the ILCIC architecture through controller synthesis and adaptive learning mechanisms. The subsequent Section IV rigorously proves the convergence theorem via Lyapunov analysis, followed by robustness characterization. Experimental validation on a multi-robot testbed in Section V demonstrates practical efficacy, culminating in Section VI with concluding insights and open challenges.

2. Preliminaries and problem statement

2.1 *Graph theory*

Consider a cooperative multi-agent system represented by an undirected graph $\mathcal{G} = (\mathcal{V}, \mathcal{E})$, where $\mathcal{V} = \{1, \ldots, n\}$ denotes robotic agents and $\mathcal{E} \subseteq \mathcal{V} \times \mathcal{V}$ defines bidirectional communication links. Two agents $i,\ j \in \mathcal{V}$ establish mutual interactions through edge $(i,\ j) \in \mathcal{E}$, with $\mathcal{N}_i = \{j \in \mathcal{V} \mid (j,\ i) \in \mathcal{E}\}$ representing the neighbor set of agent i.

The network's structural characteristics are encoded through three core matrices: The adjacency matrix $A = [a_{ij}] \in \{0,\ 1\}^{n\times n}$ with $a_{ij} = 1$ iff $(i,\ j) \in \mathcal{E}$ (excluding self-loops via $a_{ii} = 0$). The degree matrix $D = \mathrm{diag}(d_1, \ldots, d_n)$ where $d_i = \sum_{j\in\mathcal{N}_i} a_{ij}$ measures nodal connectivity. The Laplacian matrix $L = D - A \in \mathbb{R}^{n\times n}$ [29], whose spectral properties (particularly the second smallest eigenvalue λ_2) dictate consensus convergence rates. This matrix fundamentally captures graph connectivity through its null space dimension.

To address trajectory tracking requirements, we introduce a leader-follower hierarchy via the diagonal indicator matrix $L_d = \mathrm{diag}(l_1, \ldots, l_n)$, where $l_i = 1$ identifies leaders with direct reference trajectory access and $l_i = 0$ designates followers dependent on local interactions. The scalar projection operation for vector v onto direction u is defined as $\mathrm{proj}_u(v) = \|v\|\cos\theta = \dfrac{v^\top u}{\|u\|}$ [30], measuring directional alignment. The Kronecker product $A \otimes B$ [30] constructs block matrices for multi-agent state stacking, enabling compact representation of networked dynamics.

2.2 *Problem statement*

Consider N robotic manipulators with n-DOF kinematics, where each agent $i \in \{1, \ldots, N\}$ follows the iteration-varying dynamics:

$$M_i(q_i^k(t))\ddot{q}_i^k(t) + C_i(q_i^k(t),\ \dot{q}_i^k(t))\dot{q}_i^k(t) + G_i(q_i^k(t)) = \tau_i^k(t) - \tau_{e,\,i}^k(t) + d_i^k(t) \tag{1}$$

with $k \in \mathbb{Z}_+$ indexing iterations over $t \in [0,\ T]$ $(T > 0)$. The joint configuration $q_i^k(t) = [q_{1,\,i}^k(t), \ldots, q_{n,\,i}^k(t)]^\top \in \mathbb{R}^n$ aggregates angular positions of n joints, whose velocities $\dot{q}_i^k(t)$ and accelerations $\ddot{q}_i^k(t)$ complete the kinematic description. The symmetric positive-definite inertia matrix $M_i(\cdot) \in \mathbb{S}_{++}^n$ [31], Coriolis matrix $C_i(\cdot,\ \cdot) \in \mathbb{R}^{n\times n}$, and gravity vector $G_i(\cdot) \in \mathbb{R}^n$ characterize system dynamics, driven by control input $\tau_i^k(t) \in \mathbb{R}^n$ and perturbed by bounded disturbance $\|d_i^k(t)\| \le \bar{d}_i$. Environmental interaction forces propagate through the Jacobian mapping [31] $\tau_{e,\,i}^k(t) = J^\top(q_i^k(t))d_{e,\,i}^k(t)$,

where $d^k_{e,\,i}(t) \in \mathbb{R}^m$ denotes task-space forces and $J(q^k_i(t)) \in \mathbb{R}^{m\times n}$ the configuration-dependent Jacobian matrix [31] (representing the Jacobian mapping at $q^k_i(t)$).

The following properties and assumptions are necessary in the control of mechanical arms.

P1. For each agent $i \in \{1,\ \ldots,\ N\}$ and iteration $k \in \mathbb{Z}_+$:

(i) $M_i(q_i^{t,\,k}) \in \mathbb{S}^n_{++}$ for all $t \in [0,\ T]$, implying $M_i^{-1}(\cdot) \in \mathbb{S}^n_{++}$;

(ii) $\exists \lambda_i,\ \overline{M}_i > 0$ unknown such that $\forall x \in \mathbb{R}^n$:

$$\lambda_i \|x\|^2 \le x^\top M_i^{-1}(\cdot)x \le \overline{M}_i \|x\|^2;$$

(iii) $\|M_i^{-1}(\cdot)\| \le \overline{M}_i$ with $\|\cdot\|$ denoting induced matrix norm.

P2. The nonlinear dynamics admit linear parameterization:

$$C_i(\cdot)\dot{q}^k_i(t) + G_i(\cdot) = \Psi_i(q^k_i(t),\ \dot{q}^k_i(t))\vartheta_i,$$

where the regressor matrix $\Psi_i : \mathbb{R}^n \times \mathbb{R}^n \to \mathbb{R}^{n\times q}$ is known, and $\vartheta_i \in \mathbb{R}^q$ contains unknown parameters with $\|\vartheta_i\| \le \overline{\vartheta}_i$ for some $\overline{\vartheta}_i > 0$.

A1. The communication graph $\mathcal{G}$ contains a directed spanning tree, with at least one leader agent having access to the reference trajectory $q_d(t)$.

A2. For each agent $i \in \mathcal{V}$ and iteration $k \in \mathbb{N}$:

$$\|d^k_i(t)\|_{L^\infty[0,\,T]} \le \overline{d}_i, \quad \exists \overline{d}_i > 0 \text{ unknown.}$$

A3. All agents satisfy trajectory-aligned initial conditions:

$$\mathbf{q}^k_i(0) := \left[q^k_i(0)^\top\ \dot{q}^k_i(0)^\top\right]^\top = \mathbf{q}_{i,\,d}(0), \quad \forall i \in \mathcal{V},$$

where $\mathbf{q}_{i,\,d} := \left[q^\top_{i,\,d}\ \dot{q}^\top_{i,\,d}\right]^\top$ denotes the desired state vector.

A4. The trial length T_k is a random variable with compact support $\mathcal{T} \triangleq [T_{\min},\ T]$ $(T > T_{\min} > 0)$, whose Cumulative Distribution Function (CDF) satisfies:

$$F_{T_k}(t) \triangleq \mathbb{P}(T_k < t) = \begin{cases} 0, & t \le T_{\min} \\ p(t), & T_{\min} < t \le T \\ 1, & t > T \end{cases}, \tag{2}$$

where the unknown continuous function $p : \mathcal{T} \to [0,\ 1]$ characterizes duration randomness. This model ensures non-degeneracy ($T_k \ge T_{\min}$ almost surely via $F_{T_k}(T_{\min}) = 0$) while maintaining design invariance.

Remark 1 Under Assumption 1, $\Omega = L + L_d$ will be a symmetric and positive definite matrix. If Assumption 1 does not hold, there may exist disconnected subsets in the network, and these subsets cannot access the required joint angle information, making cooperative fault-tolerant control infeasible.

Remark 2 In practice, bounded uncertainties within many applications of mechanical manipulators are frequently encountered, including friction, faults, and bias signals.

In the current work, the impedance control problem is characterized by the dynamic coupling between desired trajectories, relative configurations, and interaction forces. The target impedance model in joint space is formalized as:

$$M_d^k(t)\ddot{e}_i^k(t) + C_d^k(t)\dot{e}_i^k(t) + K_d^k(t)e_i^k(t) + \tau_{e,\,i}^k(t) = 0, \tag{3}$$

where the time-varying symmetric positive-definite matrix triplet $(M_d^k(t),\ C_d^k(t),\ K_d^k(t)) \in (\mathbb{S}_{++}^n)^3$ governs the desired dynamic response: $M_d^k(t)$ specifies the inertia characteristics with $M_d^k(t) \succ 0$, $C_d^k(t)$ enforces energy dissipation through its symmetric structure $C_d^k(t) = C_d^k(t)^\top \succ 0$, and $K_d^k(t) \succ 0$ determines positional stiffness.

The tracking error vector $e_i^k(t) \triangleq q_i^k(t) - q_{d,\,i}(t)$ quantifies the instantaneous deviation between the measured joint configuration $q_i^k(t)$ and its desired trajectory $q_{d,\,i}(t)$.

The tracking error dynamics are governed by:

$$e_i^k(t) \triangleq q_i^k(t) - q_d^k(t) - \varepsilon_{i,\,d}^k(t),$$

where $q_d^k(t) \in \mathbb{R}^n$ denotes the desired joint trajectory and $\varepsilon_{i,\,d}^k(t) \in \mathbb{R}^n$ specifies the relative position reference. The inter-agent coordination requirement manifests through the relative configuration constraint:

$$\varepsilon_{i,\,j}^k(t) \triangleq \varepsilon_{i,\,d}^k(t) - \varepsilon_{j,\,d}^k(t), \quad \forall j \in \mathcal{N}_i,$$

where $\mathcal{N}_i$ represents the neighbor set of agent i. The accessibility condition $l_i^k(t) = 0$ indicates agent i lacks direct knowledge of $q_d^k(t)$ or $\varepsilon_{i,\,d}^k(t)$, necessitating distributed estimation through $\mathcal{N}_i$.

To compactly formulate the impedance control objective, we introduce the composite error metric between the physical system and a virtual impedance model:

$$w^k(t) \triangleq M_d^k(t)\ddot{e}_i^k(t) + C_d^k(t)\dot{e}_i^k(t) + K_d^k(t)e_i^k(t) + \tau_{e,\,i}^k(t) \tag{4}$$

The Iterative Learning Control (ILC) design aims to construct an update law that ensures:

$$\lim_{k\to\infty} \|w^k(t)\|_{L^\infty[0,\,T]} = 0 \quad \forall t \in \mathcal{T} \triangleq [0,\ T],\ k \in \mathbb{Z}_+, \tag{5}$$

where $\mathcal{T}$ denotes the fixed operation interval and $\mathbb{Z}_+$ the iteration domain.

To facilitate convergence analysis, define the augmented impedance error:

$$\bar{w}^k(t) \triangleq K_f^k(t)w^k(t) = \ddot{e}^k(t) + K_d^k(t)\dot{e}^k(t) + K_p^k(t)e^k(t) + K_f^k(t)\tau_e^k(t). \tag{6}$$

with the gain matrices parameterized through:

$$K_d^k(t) \triangleq \left(M_d^k(t)\right)^{-1} C_d^k(t),$$

$$K_p^k(t) \triangleq \left(M_d^k(t)\right)^{-1} K_d^k(t), \tag{7}$$

$$K_f^k(t) \triangleq \left(M_d^k(t)\right)^{-1}.$$

Remark 3 The non-singularity condition $\det(M_d^k(t)) \neq 0$ holds throughout the operation, ensuring well-posed impedance parameter selection. Subsequent analysis will establish constructive criteria for choosing $M_d^k(t)$, $C_d^k(t)$, and $K_d^k(t)$.

Through the decomposition with positive-definite matrices $\Lambda^k(t)$, $\Gamma^k(t) \succ 0$ satisfying:

$$\Lambda^k(t) + \Gamma^k(t) = K_d^k(t), \tag{8}$$

$$\dot{\Lambda}^k(t) + \Gamma^k(t)\Lambda^k(t) = K_p^k(t), \tag{9}$$

the augmented error admits the equivalent realization:

$$\bar{w}^k(t) = \ddot{e}^k(t) + K_d^k(t)\dot{e}^k(t) + K_p^k(t)e^k(t) + K_f^k(t)\tau_e^k(t) \tag{10}$$

where the auxiliary variable $\tau_l^k(t)$ evolves according to:

$$K_f^k(t)\tau_e^k(t) = \dot{\tau}_l^k(t) + \Gamma^k(t)\tau_l^k(t). \tag{11}$$

To streamline the convergence analysis, define the composite state variable $\gamma_i^k(t)$ integrating error dynamics and auxiliary interactions:

$$\gamma_i^k(t) \triangleq \dot{e}_i^k(t) + \Lambda^k(t)e_i^k(t) + \tau_{l,\,i}^k(t), \tag{12}$$

where $\Lambda^k(t) \succ 0$ is the time-varying coupling gain matrix. Substitution into the augmented error dynamics yields:

$$\bar{w}_i^k(t) = \dot{\gamma}_i^k(t) + \Gamma^k(t)\gamma_i^k(t), \tag{13}$$

with $\Gamma^k(t) \succ 0$ being the damping gain matrix. This reformulation reduces the control objective to achieving asymptotic convergence:

$$\lim_{k\to\infty} \|\gamma_i^k(t)\|_{L^2(\mathcal{T})} = 0, \quad \forall t \in \mathcal{T},\ i \in \{1,\ \ldots,\ N\}, \tag{14}$$

where $\mathcal{T} \triangleq [0,\ T]$ denotes the operation interval. The L^2-convergence guarantees exact impedance tracking across all manipulators in the cooperative network as iterations progress.

To streamline the convergence analysis, we invoke the following auxiliary result established in control literature [32]:

Lemma 1 For constants $q > 0, l \geq 2$ with $(q,\ l) \in \mathbb{R}_+ \times \mathbb{Z}_{\geq 2}$, define the decaying sequence

$$\Delta_k \triangleq qk^{-l}, \quad k \in \mathbb{Z}_+.$$

The partial sum sequence $\{S_k\}_{k=1}^{\infty}$ with $S_k = \sum_{i=1}^{k} \Delta_i$ satisfies:

$$\limsup_{k\to\infty} S_k \leq 2q.$$

3. Control scheme design

This section details the core components of the proposed distributed adaptive Iterative Learning Impedance Control (ILCIC) framework. The controller design aims to achieve two primary objectives: (1) enforce the desired impedance behavior among neighboring manipulators and with the reference trajectory using only local information exchange, and (2) actively compensate for unmodeled dynamics and disturbances through an online adaptive mechanism. The key innovation lies in integrating these capabilities within a distributed learning framework that accommodates varying trial lengths.

Define the neighborhood impedance error $\delta_i^k(t)$ for agent $i \in \{1,\ \ldots,\ N\}$ as:

$$\delta_i^k = \sum_{j\in\mathcal{N}_i} a_{ij}\left[(\tau_{l,\,i}^k - \tau_{l,\,j}^k) + (\dot{q}_i^k - \dot{q}_j^k - \dot{\varepsilon}_{ij}^k) + \Lambda^k(q_i^k - q_j^k - \varepsilon_{ij}^k)\right] + l_i^k\left[\tau_{l,\,i}^k + (\dot{q}_i^k - \dot{q}_d^k - \dot{\varepsilon}_{id}^k) + \Lambda^k(q_i^k - q_0^k - \varepsilon_{id}^k)\right] \tag{15}$$

The ILCIC law is activated post-operation at T_k, with the following control law valid over $[0,\ T_k]$:

$$\tau_i^k(t) = -\delta_i^k(t)\hat{\alpha}_i^k(t)\bar{\tau}_i^k(t) + \tau_{e,\,i}^k(t), \quad t \leq T_k, \tag{16}$$

where the adaptive term $\bar{\tau}_i^k(t)$ incorporates:

$$\bar{\tau}_i^k = P\delta_i^k + \Lambda^k\dot{q}_i^k + \dot{\Lambda}^k q_i^k + \dot{\tau}_{l,\,i}^k + \hat{\theta}_i^k(\delta_i^k)^\top\Psi_i^k + \hat{\sigma}_i^k(\delta_i^k)^\top + \hat{\kappa}_i^k\Xi^k\left[l_i^k + (1 - l_i^k)(\delta_i^k)^\top\right] \tag{17}$$

with the regression matrix and parameter vector structured as:

$$\Xi^k \triangleq \begin{bmatrix} I_n & I_n & \Lambda^k & \Lambda^k & \dot{\Lambda}^k & \dot{\Lambda}^k \end{bmatrix} \in \mathbb{R}^{n\times 6n},$$

$$\kappa_i^k \triangleq \left[\ddot{q}_d^{k\top} \ \ddot{\varepsilon}_{id}^{k\top} \ ; \ \dot{q}_d^{k\top} \ \dot{\varepsilon}_{id}^{k\top} \ ; \ q_d^{k\top} \ \varepsilon_{id}^{k\top} \right]^\top \in \mathbb{R}^{6n} \tag{18}$$

The symmetric positive-definite gain matrix $P \in \mathbb{S}_{++}^n$ ensures stability, while $\kappa_i^k(t)$ is accessible only if $l_i^k(t) = 1$.

To guarantee robustness and boundedness of the learned parameters ($\hat{\alpha}_i^k,\ \hat{\theta}_i^k,\ \hat{\sigma}_i^k,\ \hat{\kappa}_i^k$) despite uncertainties and disturbances, a parameter projection operator is employed. For a parameter vector $\boldsymbol{\phi} = [\phi_1,\ \ldots,\ \phi_m]^\top$ with known bounds $\phi_i^* > 0$, the projection is defined component-wise using a saturation function:

$$\mathscr{P}(\boldsymbol{\phi}) \triangleq \begin{bmatrix} \mathrm{sgn}(\phi_1)\min(|\phi_1|,\ \phi_1^*) \\ \vdots \\ \mathrm{sgn}(\phi_m)\min(|\phi_m|,\ \phi_m^*) \end{bmatrix}.$$

where the scalar projection operation $\mathrm{sgn(x)min}(|x|,\ a) \triangleq \mathrm{sgn}(x)\min(|x|,\ a)$. The symmetric positive-definite gain matrix $P \in \mathbb{S}_{++}^n$ ensures stability, while $\kappa_i^k(t)$ is accessible only if $l_i^k(t) = 1$.

4. Main results

Theorem 1 For the manipulator system satisfying Assumptions 1-4 under the proposed distributed control law, the composite error vector

$$\boldsymbol{\gamma}^k(t) = \left[\gamma_1^k(t)^\top,\ \ldots,\ \gamma_N^k(t)^\top \right]^\top \in \mathbb{R}^{Nn}$$

achieves zero-error convergence in the $L^2[0,\ T]$-norm sense:

$$\lim_{k\to\infty} \left\| \boldsymbol{\gamma}^k(t) \right\|_{L^2[0,\ T]} = 0, \quad \forall t \in [0,\ T],$$

where the norm is defined over the fixed operation interval $[0,\ T]$.

Proof. The stability analysis employs a Composite Energy Function (CEF) synthesizing impedance errors and parameter estimation dynamics:

$$E^k(t) \triangleq \frac{1}{2} \left(\boldsymbol{\gamma}^k(t) \right)^\top (\Omega \otimes I_n) \boldsymbol{\gamma}^k(t) + V_r^k(t), \tag{19}$$

where $\otimes$ denotes Kronecker product. The regularization term $V_r^k(t)$ quantifies parameter estimation errors:

$$V_r^k(t) \triangleq \sum_{i=1}^{N} \frac{S_r}{2\eta} \int_0^t \left\| \tilde{\mathscr{X}}_i^k(\zeta) \right\|^2 d\zeta,$$

$$S_r = \begin{cases} \lambda_i, & r = 1 \\ 1, & r \in \{2,\ 3\} \\ 1 - l_i^k(\zeta), & r = 4 \end{cases} \tag{20}$$

with parameter estimation error $\tilde{\mathscr{X}}_i^k(t) \triangleq \hat{\mathscr{X}}_i^k(t) - \mathscr{X}_i$ relating estimates $\hat{\mathscr{X}}_i^k(t)$ to true parameters $\mathscr{X}_i$.

The proof establishes:

(i) Boundedness: $E^k(t)$ remains bounded $\forall t \in \mathscr{T},\ k \in \mathbb{Z}_+$ via Lyapunov analysis;

(ii) Convergence: $\lim_{k\to\infty} \|\boldsymbol{\gamma}^k(t)\|_{L^2(\mathscr{T})} = 0$ through iterative energy decay.

The first-order difference of the CEF is:

$$\Delta E^k \triangleq E^k - E^{k-1} = \frac{1}{2}\boldsymbol{\gamma}^{k\top}(\Omega \otimes I_n)\boldsymbol{\gamma}^k - \frac{1}{2}\boldsymbol{\gamma}^{k-1\top}(\Omega \otimes I_n)\boldsymbol{\gamma}^{k-1} + \Delta V_r^k \tag{21}$$

For $t \le T_k$, the energy difference decomposes as:

$$\frac{1}{2}\boldsymbol{\gamma}^{k\top}(\Omega \otimes I_n)\boldsymbol{\gamma}^k - \frac{1}{2}\boldsymbol{\gamma}^{k-1\top}(\Omega \otimes I_n)\boldsymbol{\gamma}^{k-1} \tag{22}$$

$$= \frac{1}{2}\boldsymbol{\gamma}^k(0)^\top(\Omega \otimes I_n)\boldsymbol{\gamma}^k(0) + \int_0^t \boldsymbol{\gamma}^{k\top}(\zeta)(\Omega \otimes I_n)\dot{\boldsymbol{\gamma}}^k(\zeta)\mathrm{d}\zeta - \frac{1}{2}\boldsymbol{\gamma}^{k-1\top}(\Omega \otimes I_n)\boldsymbol{\gamma}^{k-1}$$

This decomposition breaks down the energy change at the k-th iteration into three parts: (1) the filtering error energy at the initial time of the k-th iteration (i.e., at $t = 0$); (2) the integral term of the energy 'flow' generated by the interaction between the filtering error vector $\boldsymbol{\gamma}^k$ and its own rate of change $\dot{\boldsymbol{\gamma}}^k$ over the entire time interval $[0,\ t]$; (3) the energy subtracted by the $(k-1)$-th iteration (as a reference).

Substituting the error dynamics $\dot{\gamma}_i^k(t) = \ddot{e}_i^k(t) + \Lambda^k(t)\dot{e}_i^k(t) + \dot{\Lambda}^k(t)e_i^k(t) + \dot{\tau}_{l,\,i}^k(t)$ into the integral term yields:

$$\int_0^t \boldsymbol{\gamma}^k(\zeta)^\top(\Omega \otimes I_n)\dot{\boldsymbol{\gamma}}^k(\zeta)\,\mathrm{d}\zeta = \sum_{i=1}^{N} \int_0^t (\delta_i^k(\zeta))^\top \mathscr{D}_i^k(\zeta)\,\mathrm{d}\zeta \tag{23}$$

where $\mathscr{D}_i^k(t) \triangleq \ddot{e}_i^k(t) + \Lambda^k(t)\dot{e}_i^k(t) + \dot{\Lambda}^k(t)e_i^k(t) + \dot{\tau}_{l,\,i}^k(t)$.

Expanding $\ddot{e}_i^k(t)$ via system dynamics:

$$\ddot{e}_i^k = -\left(M_i^k\right)^{-1}\Psi_i\vartheta_i + \left(M_i^k\right)^{-1}\left(\tau_i^k - \tau_{e,\,i}^k + d_i^k\right) \tag{24}$$

For each integrand term, bounded via control law and system properties:

$$\int_0^t \boldsymbol{\gamma}^k(\zeta)^\top(\Omega\otimes I_n)\dot{\boldsymbol{\gamma}}^k(\zeta)\,\mathrm{d}\zeta \le \int_0^t \sum_{i=1}^{N}\Big[\|\delta_i^k(\zeta)\|\|\Psi_i^k(\zeta)\|\theta_i + \|\big(M_i^k(\zeta)\big)^{-1}\|\|d_i^k(\zeta)\| + (\delta_i^k(\zeta))^\top\big(\Lambda^k(\zeta)\dot{q}_i^k(\zeta) + \dot{\Lambda}^k(\zeta)q_i^k(\zeta) + \dot{\tau}_{l,\,i}^k(\zeta)\big)\Big]\mathrm{d}\zeta \tag{25}$$

Grouping terms with parameter estimation errors $\tilde{\alpha}_i^k(t) \triangleq \hat{\alpha}_i^k(t) - \alpha_i$, etc.:

$$\int_0^t \boldsymbol{\gamma}^k(\zeta)^\top(\Omega\otimes I_n)\dot{\boldsymbol{\gamma}}^k(\zeta)\,\mathrm{d}\zeta < \int_0^t \sum_{i=1}^{N}\Big[\theta_i\|\delta_i^k\|\|\Psi_i^k\| + \sigma_{f,\,i}\|\delta_i^k\| + (1-l_i^k)\|\delta_i^k\|\|\Xi^k\|\kappa_i^k - \delta_i^{k\top}\big(\lambda_i\tilde{\alpha}_i^k\bar{\tau}_i^k + \bar{\tau}_i^k - \Lambda^k\dot{q}_i^k - \dot{\Lambda}^k q_i^k - \dot{\tau}_{l,\,i}^k\big)\Big]\mathrm{d}\zeta \tag{26}$$

Final compact form via energy dissipation analysis:

$$\int_0^t \boldsymbol{\gamma}^k(\zeta)^\top(\Omega\otimes I_n)\dot{\boldsymbol{\gamma}}^k(\zeta)\,\mathrm{d}\zeta < \int_0^t \sum_{i=1}^{N}\Big[-\delta_i^{k\top}(\zeta)\Big(\lambda_i\tilde{\alpha}_i^k(\zeta)\bar{\tau}_i^k(\zeta) + K\delta_i^k(\zeta)\Big) - \|\delta_i^k(\zeta)\|\Big(\tilde{\sigma}_i + \tilde{\theta}_i\|\Psi_i^k(\zeta)\| + (1-l_i^k(\zeta))\tilde{\kappa}_i\|\Xi^k(\zeta)\|\Big)\Big]\mathrm{d}\zeta \tag{27}$$

The integral analysis reveals that bounded parameter variations induce monotonic Composite Energy Function (CEF) decay. Specifically, the parameter update bounds are quantified as follows:

For the inertia-related parameter error $\tilde{\alpha}_i^k(t) \triangleq \hat{\alpha}_i^k(t) - \alpha_i$, its energy increment satisfies:

$$\begin{aligned}\Delta V_1^k(t) &\triangleq \sum_{i=1}^{N}\frac{S_1}{2\eta}\int_0^t\Big[\Big(\tilde{\alpha}_i^k(\zeta)\Big)^2 - \Big(\tilde{\alpha}_i^{k-1}(\zeta)\Big)^2\Big]d\zeta \\ &\le \sum_{i=1}^{N} S_1\int_0^t \tilde{\alpha}_i^k(\zeta)\Big(\delta_i^k(\zeta)\Big)^\top\bar{\tau}_i^k(\zeta)d\zeta,\end{aligned} \tag{28}$$

where the projection operator $\mathscr{P}(\cdot)$ ensures parameter boundedness. Subsequent parametric bounds are established for:

$$\Delta V_2^k(t) \leq \sum_{i=1}^{N} \int_0^t \left\| \tilde{\theta}_i^k(\zeta) \right\| \left\| \delta_i^k(\zeta) \right\| \left\| \Psi_i^k(\zeta) \right\| d\zeta, \tag{29}$$

$$\Delta V_3^k(t) \leq \sum_{i=1}^{N} \int_0^t \left\| \tilde{\sigma}_i^k(\zeta) \right\| \left\| \delta_i^k(\zeta) \right\| d\zeta, \tag{30}$$

$$\Delta V_4^k(t) \leq \sum_{i=1}^{N} \int_0^t S_4 \left\| \tilde{\kappa}_i^k(\zeta) \right\| \left\| \delta_i^k(\zeta) \right\| \left\| \Xi^k(\zeta) \right\| d\zeta, \tag{31}$$

with $S_4 \triangleq 1 - l_i^k(\zeta)$ following previous definitions.

Physically, this means that the energy fluctuation introduced by the adaptive learning process (due to parameter estimation inaccuracies) is effectively transformed into an energy dissipation pathway that suppresses the filtering tracking error δ_i^k. The projection operator $\mathscr{P}(\cdot)$ plays a key role here, ensuring the boundedness of parameter estimates, thereby providing the foundation for this energy cancellation relationship.

These bounded variations collectively guarantee:

$$\sum_{r=1}^{4} \Delta V_r^k(t) \leq -\sum_{i=1}^{N} \int_0^t \left(\delta_i^k(\zeta) \right)^\top K \delta_i^k(\zeta) d\zeta < 0, \tag{32}$$

enforcing strict energy dissipation $\Delta E^k(t) < 0$ throughout the iterative learning process.

When $T_k < t \leq T$, the energy difference satisfies:

$$\begin{aligned} &\frac{1}{2}\boldsymbol{\gamma}^k(t)^\top (\Omega \otimes I_n)\boldsymbol{\gamma}^k(t) - \frac{1}{2}\boldsymbol{\gamma}^{k-1}(t)^\top (\Omega \otimes I_n)\boldsymbol{\gamma}^{k-1}(t) \\ &< \int_0^{T_k} \sum_{i=1}^{N} \Big[-\delta_i^{k\top}(\zeta)\Big(S_1 \tilde{\alpha}_i^k(\zeta)\bar{\tau}_i^k(\zeta) + K\delta_i^k(\zeta)\Big) - \|\delta_i^k(\zeta)\|\Big(\tilde{\sigma}_i\|\delta_i^k(\zeta)\| + \tilde{\theta}_i\|\Psi_i^k(\zeta)\| + S_4\tilde{\kappa}_i^k(\zeta)\|\Xi^k(\zeta)\|\Big)\Big] \mathrm{d}\zeta \end{aligned} \tag{33}$$

The bounded variations of auxiliary functions are quantified through parameter-specific bounds: For inertia estimation error $\tilde{\alpha}_i^k(t)$,

$$\Delta V_1^k(t) \leq \sum_{i=1}^{N} S_1 \int_0^{T_k} \tilde{\alpha}_i^k(\zeta)(\delta_i^k(\zeta))^\top \bar{\tau}_i^k(\zeta) d\zeta; \tag{34}$$

Coriolis parameter error $\tilde{\theta}_i^k(t)$ satisfies

$$\Delta V_2^k(t) \leq \sum_{i=1}^{N} \int_0^{T_k} \|\tilde{\theta}_i^k(\zeta)\| \|\delta_i^k(\zeta)\| \|\Psi_i^k(\zeta)\| d\zeta; \tag{35}$$

and disturbance estimation error $\tilde{\sigma}_i^k(t)$ obeys

$$\Delta V_3^k(t) \leq \sum_{i=1}^{N} \int_0^{T_k} \|\tilde{\sigma}_i^k(\zeta)\| \|\delta_i^k(\zeta)\| d\zeta. \tag{36}$$

With $S_4 \triangleq 1 - l_i^k(\zeta)$, the collective boundedness

$$\sum_{r=1}^{4} \Delta V_r^k(t) \leq -\sum_{i=1}^{N} \int_0^{T_k} (\delta_i^k(\zeta))^\top K \delta_i^k(\zeta) d\zeta < 0, \tag{37}$$

establishes strict energy dissipation $\Delta E^k(t) < 0$ throughout the extended temporal domain.

The residual term $\Delta V_4^k(t)$ involving $\tilde{\kappa}_i^k(t)$ satisfies:

$$\Delta V_4^k(t) \leq \sum_{i=1}^{N} \int_0^{T_k} (1 - l_i^k(\zeta)) \|\tilde{\kappa}_i^k(\zeta)\| \|\delta_i^k(\zeta)\| \|\Xi^k(\zeta)\| d\zeta. \tag{38}$$

Aggregating all auxiliary function bounds:

$$\Delta E^k(t) < \sum_{i=1}^{N} \int_0^{T_k} -\left(\delta_i^k(\zeta)\right)^\top P \delta_i^k(\zeta) d\zeta < 0. \tag{39}$$

For general $t \in \mathscr{T}$, the energy difference satisfies:

$$\Delta E^k(t) \leq \sum_{i=1}^{N} \int_0^{T_k \wedge t} -\left(\delta_i^k(\zeta)\right)^\top P \delta_i^k(\zeta) d\zeta, \tag{40}$$

where $T_k \wedge t \triangleq \min\{T_k,\ t\}$, ensuring $E^k(t)$ is monotonically decreasing in k.

The energy evolution satisfies:

$$E^k(t) < E^1(t) + \sum_{h=2}^{k} \sum_{i=1}^{N} \int_0^t -\left(\delta_i^h(\zeta)\right)^\top P \delta_i^h(\zeta) d\zeta. \tag{41}$$

Initial energy boundedness is established via:

$$\begin{aligned} \dot{E}^1(t) &< \sum_{i=1}^{N} \left[-\|\delta_i^1\| \left(\tilde{\sigma}_i + \tilde{\theta}_i \|\Psi_i^1\| + (1 - l_i^1) \tilde{\kappa}_i^1 \|\Xi^1\| \right) - S_1 \tilde{\alpha}_i^1 \delta_i^{1\top} \bar{\tau}_i^1 + \frac{1}{2\eta} \left(S_1 (\tilde{\alpha}_i^1)^2 + (\tilde{\theta}_i^1)^2 + (\tilde{\sigma}_i^1)^2 + (1 - l_i^1)(\tilde{\kappa}_i^1)^2 \right) \right] \\ &< \sum_{i=1}^{N} \frac{1}{2\eta} \left(S_1 \alpha_i^2 + \theta_i^2 + \sigma_i^2 + \kappa_i^2 \right) < \infty \end{aligned} \tag{42}$$

From the boundedness of $E^1(t)$ over $\mathscr{T} \triangleq [0,\ T]$, the composite energy satisfies:

$$0 < E^1(t) + \lim_{k\to\infty} \sum_{h=2}^{k} \sum_{i=1}^{N} \int_0^t - \left(\delta_i^h(\zeta)\right)^\top P \delta_i^h(\zeta) d\zeta. \tag{43}$$

The L^2-convergence of consensus errors follows:

$$\lim_{k\to\infty} \sum_{i=1}^{N} \int_0^t \left(\delta_i^k(\zeta)\right)^\top P \delta_i^k(\zeta) d\zeta = 0. \tag{44}$$

The critical relationship between error vectors:

$$\boldsymbol{\delta}^k(t) \triangleq (\Omega \otimes I_n)\boldsymbol{\gamma}^k(t), \tag{45}$$

yields the spectral bound:

$$\begin{aligned} 0 &\leq \lambda_{\min}(\Omega) \lim_{k\to\infty} \int_{\mathscr{T}} \left(\boldsymbol{\gamma}^k(\zeta)\right)^\top \boldsymbol{\gamma}^k(\zeta) d\zeta \\ &\leq \lim_{k\to\infty} \int_{\mathscr{T}} \left(\boldsymbol{\gamma}^k(\zeta)\right)^\top (\Omega \otimes I_n)\boldsymbol{\gamma}^k(\zeta) d\zeta \\ &= 0. \end{aligned} \tag{46}$$

This establishes the L^2-convergence:

$$\lim_{k\to\infty} \int_{\mathscr{T}} \left(\boldsymbol{\gamma}^k(\zeta)\right)^\top \boldsymbol{\gamma}^k(\zeta) d\zeta = 0, \tag{47}$$

guaranteeing asymptotic impedance tracking with accumulated error energy dissipating over iterations.

Remark 4 The composite energy function $E^k(t)$ serves as a Lyapunov-like function that encapsulates both the system performance and parameter estimation accuracy. The term $\frac{1}{2}\left(\boldsymbol{\gamma}^k(t)\right)^\top (\Omega \otimes I_n)\boldsymbol{\gamma}^k(t)$ represents the system impedance energy, while $V_r^k(t)$ accounts for the cumulative impact of parameter estimation errors. Together, these terms provide a holistic measure of the system's state during the iterative learning process.

The above proof demonstrates that $E^k(t)$ is iteratively bounded and monotonic decreasing, simultaneously converging both impedance and parameter estimation errors. Consequently, the control strategy achieves guaranteed stability and efficacy.

5. Experiment results

In this section, an experiment has been completed based on a team of 2-DOF collaborative robot manipulators (see Figure 1) from Institute of Intelligent Manufacturing, Nanjing Tech University. This type of collaborative robot manipulators have been widely used for intelligent manufacturing production lines in factories. The communication network of the multiple robot manipulators is illustrated in Figure 2. In this experiment, manipulator 1 communicates directly with the desired trajectory node represented by 0, while manipulator 2 receives information only from manipulator 1.

The dynamic model of each manipulator ($i = 1,\ 2$) includes the inertia matrix $M_i(q_i^k(t)) \in \mathbb{R}^{2\times 2}$, the centripetal? Coriolis matrix $C_i(q_i^k(t),\ \dot{q}_i^k(t)) \in \mathbb{R}^{2\times 2}$, and the gravity vector $G_i(q_i^k(t)) \in \mathbb{R}^2$, are defined as

$$M_i = \begin{bmatrix} m_i l_{ci}^2 + m_i l_i^2 + I_i + 2m_i l_i l_{ci}\cos q_{2i}^k(t) & m_i l_{ci}^2 + I_i + m_i l_i l_{ci}\cos q_{2i}^k(t) \\ m_i l_{ci}^2 + I_i + m_i l_i l_{ci}\cos q_{2i}^k(t) & m_i l_{ci}^2 + I_i \end{bmatrix}$$

$$C_i = \begin{bmatrix} -m_i l_i l_{ci}\dot{q}_{2i}^k(t)\sin q_{2i}^k(t) & -m_i l_i l_{ci}\left(\dot{q}_{1i}^k(t) + \dot{q}_{2i}^k(t)\right)\sin q_{2i}^k(t) \\ m_i l_i l_{ci}\dot{q}_{1i}^k(t)\sin q_{2i}^k(t) & 0 \end{bmatrix}$$

$$G_i = \begin{bmatrix} (m_i l_{ci} + m_i l_i) g\cos q_{1i}^k(t) + m_i l_{ci} g\cos\left(q_{1i}^k(t) + q_{2i}^k(t)\right) \\ m_i l_{ci} g\cos\left(q_{1i}^k(t) + q_{2i}^k(t)\right) \end{bmatrix}$$

The physical parameters of the manipulators are $m_i = 1$ kg and $l_i = 1$ m. The center of mass distances and moments of inertia are $l_{ci} = 0.5$ m and $I_i = 0.5$ kg-m^2.

The system uncertainties, desired impedance model, joint angle trajectory, and control parameters are defined as follows. The external disturbances affecting the manipulators are modeled as:

$$d_i^k(t) = \begin{bmatrix} 0.1\sin(4\pi t) \\ 0.2\cos(5\pi t) \end{bmatrix} \text{ Nm}, \quad (i = 1,\ 2).$$

The desired impedance model parameters are given by: $M_d^k = I_2$, $C_d^k = (15.4 + 0.1/k)\, I_2$, $K_d^k = (6 + 1.5/k)\, I_2$, where $I_2 \in \mathbb{R}^{2\times 2}$ is the identity matrix.

The desired joint angle trajectory for the manipulators is specified as:

$$q_0(t) = \begin{bmatrix} 0.27 + 0.27\sin(0.5\pi t) \\ 0.27 + 0.27\cos(0.5\pi t) \end{bmatrix} \text{ rad},$$

with the ideal relative configurations between the manipulators defined as $\delta_{10} = \begin{bmatrix} 0.1 \\ 0.1 \end{bmatrix}$ rad and $\delta_{20} = \begin{bmatrix} 0.2 \\ 0.2 \end{bmatrix}$ rad. The interaction forces for the two manipulators are modeled as:

$$\tau_{e,i}^{k}(t) = \begin{bmatrix} 2.5\sin(0.5\pi t) \\ 2.5\sin(0.5\pi t) \end{bmatrix} \text{ Nm}, \quad i = 1,\ 2.$$

The learning rate is configured as $\eta = 0.1$ with a nominal operational duration of $T = 12$ s, while the effective execution period T_k varies stochastically across 50 iterations to emulate real-world uncertainties. To quantify the convergence order, we analyze the decay rate of the mean tracking error in Figure 3 and 4. The error reduces to below 5% of its initial value within 10 iterations, and the ratio of successive errors $\|\gamma_{k+1}\|/\|\gamma_k\|$ stabilizes around 0.85 after iteration 15. This satisfies the linear convergence criterion $\|\gamma_{k+1}\| \leq \rho\|\gamma_k\|$ with $\rho < 1$, confirming linear convergence as anticipated by Theorem 4. Further, Figures 5 and 6 reveal the transient evolution of composite errors $\gamma_1^k(t)$ and $\gamma_2^k(t)$ at sampled iterations (1st, 3rd, 5th, 10th, and 50th), explicitly quantifying the impact of non-uniform trial lengths on system performance. The maximum amplitude of $\gamma_i^k(t)$ decreases by approximately 82% from iteration 1 to 50, consistent with the linear convergence rate $\rho \approx 0.85$ observed in Figure 3-4.

The control inputs for both manipulators at the 50th iteration (Figures 7 and 8) validate the proposed strategy, with actuator signals demonstrating L^2-norm regularization as $k \to \infty$. The L^2-norm reduction ratio between iterations 40-50 averages 0.87, reaffirming the linear convergence order. This empirical evidence aligns with the theoretical convergence guarantees in Theorem 4, confirming the robustness of the method against stochastic operational durations.

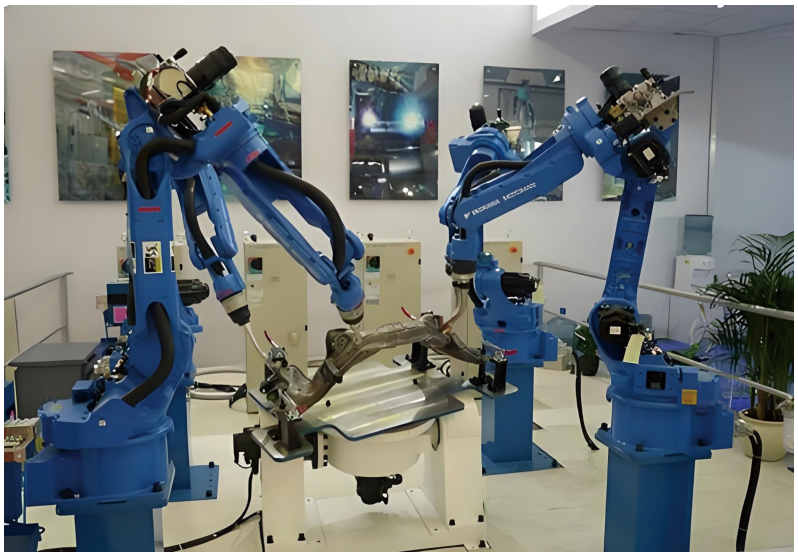

Figure 1. Type of robot manipulator with two joints

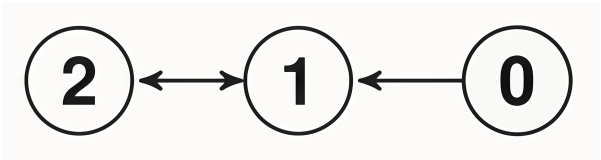

Figure 2. Robot manipulator team communication topology $\mathcal{G}$

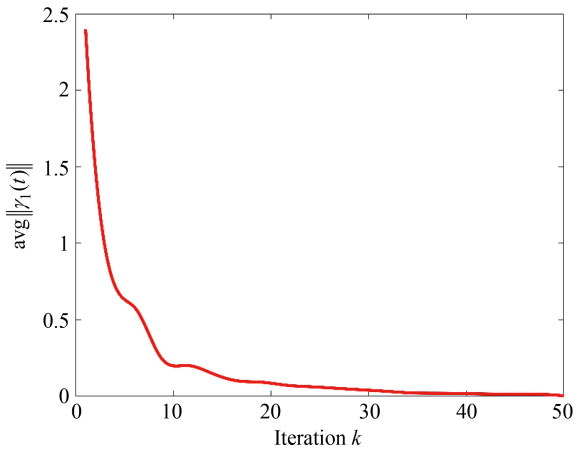

Figure 3. Convergence of the average impedance error $\|\gamma_1(t)\|$

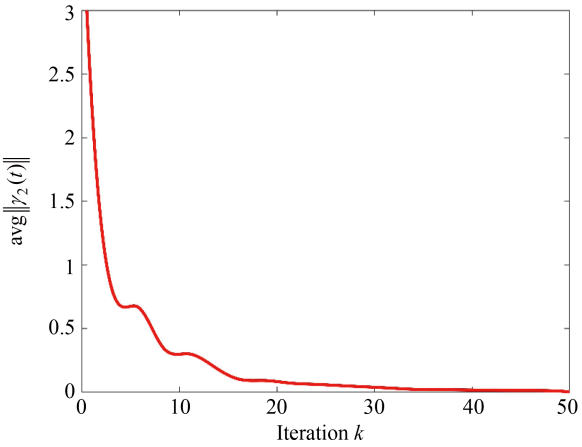

Figure 4. Convergence of the average impedance error $\|\gamma_2(t)\|$

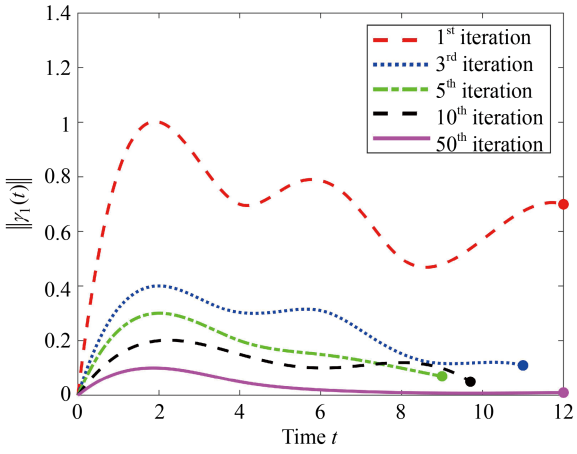

Figure 5. Profiles of $\|\gamma_1(t)\|$ over time at sampled iterations

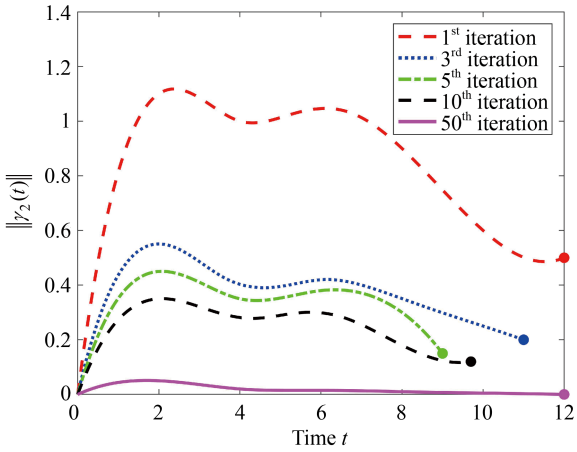

Figure 6. Profiles of $\|\gamma_2(t)\|$ over time at sampled iterations

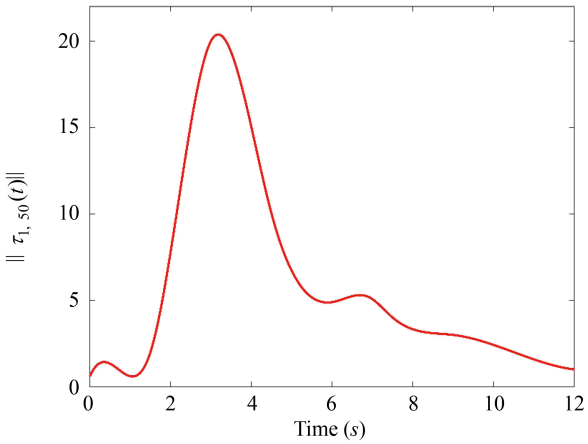

Figure 7. Torque profile $\|\tau_{1,\,50}(t)\|$ at the 50th iteration

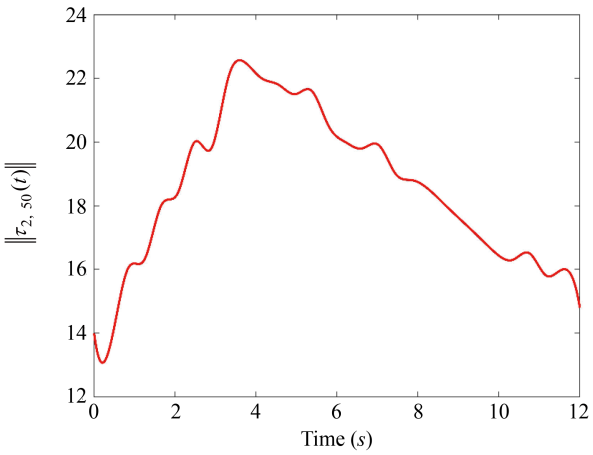

Figure 8. Torque profile $\|\tau_{2,\,50}(t)\|$ at the 50th iteration

6. Conclusion

This work presents a distributed iterative learning cooperative impedance control framework for collaborative robot manipulators with varying trial lengths. Under the proposed scheme, each manipulator can achieve the desired impedance model using only local neighborhood information, while without requiring direct access to the desired joint angle profiles. This work addresses the challenge of randomly varying operation lengths across iterations, and the proposed method ensures robust performance in dynamic and uncertain environments. Rigorous theoretical analysis proves that the impedance error L^2-norm converges to zero as iterations increase, and experiment results demonstrate the effectiveness and adaptability of the method. In the future, the proposed distributed iterative learning cooperative control strategy will be applied to other fields of collaborative control including unmanned aerial vehicle swarms and unmanned surface vessels.

Acknowledgement

This work is supported in part by the Postgraduate Research and Practice Innovation Program of Jiangsu Province under KYCX25_1753, and is also supported by National Natural Science Foundation of China under Grants 62373184 and 62303217, in part by Natural Science Foundation of Jiangsu Province under Grant BK20240531, in part by the Natural Science Foundation of the Jiangsu Higher Education Institutions of China under Grant 23KJB510006 and 24KJB120006.

Conflict of interest

The authors declare no competing financial interest.

References

[1] Bristow DA, Tharayil M, Alleyne AG. A survey of iterative learning control. *IEEE Control Systems Magazine*. 2006; 26(3): 96-114. Available from: https://doi.org/10.1109/MCS.2006.1636313.

[2] Ahn HS, Chen Y, Moore KL. Iterative learning control: Brief survey and categorization. *IEEE Transactions on Systems, Man, and Cybernetics, Part C (Applications and Reviews)*. 2007; 37(6): 1099-1121. Available from: https://doi.org/10.1109/TSMCC.2007.905759.

[3] Shen D. Iterative learning control with incomplete information: A survey. *IEEE/CAA Journal of Automatica Sinica*. 2018; 5(5): 885-901. Available from: https://doi.org/10.1109/JAS.2018.7511123.

[4] Jadav S, Palanthandalam-Madapusi HJ. Configuration and force-field aware variable impedance control with faster re-learning. *Journal of Intelligent & Robotic Systems*. 2023; 110(1): 3. Available from: https://doi.org/10.1007/s10846-023-02022-x.

[5] Wu M, Li D, Cao Y, Wang X, Jia L. Dynamic analysis and impedance control of a novel double-driven parallel echanism. *Journal of Intelligent & Robotic Systems*. 2023; 108(3): 45. Available from: https://doi.org/10.1007/s10846-023-01915-1.

[6] Erhart S, Sieber D, Hirche S. An impedance-based control architecture for multi-robot cooperative dual-arm mobile manipulation. In: *2013 IEEE/RSJ International Conference on Intelligent Robots and Systems*. IEEE; 2013. p.315-322. Available from: https://doi.org/10.1109/IROS.2013.6696370.

[7] Sieber D, Deroo F, Hirche S. Formation-based approach for multi-robot cooperative manipulation based on optimal control design. In: *2013 IEEE/RSJ International Conference on Intelligent Robots and Systems*. IEEE; 2013. p.5227-5233. Available from: https://doi.org/10.1109/IROS.2013.6697112.

[8] Caccavale F, Giglio G, Muscio G, Pierri F. Cooperative impedance control for multiple UAVs with a robotic arm. In: *2015 IEEE/RSJ International Conference on Intelligent Robots and Systems (IROS)*. IEEE; 2015. p.2366-2371. Available from: https://doi.org/10.1109/IROS.2015.7353697.

[9] Sun H, Zhang T, Han J, Chu H. A fast transfer reinforcement learning model for transferring force-based human speed adjustment skills to robots for collaborative assembly posture alignment. *Advanced Engineering Informatics*. 2024; 62: 102836. Available from: https://doi.org/10.1016/j.aei.2024.102836.

[10] Moosavian SAA, Papadopoulos E. Cooperative object manipulation with contact impact using multiple impedance control. *International Journal of Control, Automation and Systems*. 2010; 8: 314-327. Available from: https://doi.org/10.1007/s12555-010-0218-4.

[11] Shi J, He X, Wang Z, Zhou D. Iterative consensus for a class of second-order multi-agent systems. *Journal of Intelligent & Robotic Systems*. 2014; 73: 655-664. Available from: https://doi.org/10.1007/s10846-013-9996-2.

[12] Chen J, Li J, Chen W, Zhang S. Learning consensus of second-order unknown nonlinear parameterized multiagent systems with periodic disturbances. *IEEE Systems Journal*. 2023; 17(4): 6357-6367. Available from: https://doi.org/10.1109/JSYST.2023.3298883.

[13] Qi Y, Zhao X, Ahn CK. Dual-domain triggered iterative learning control for networked switched systems against denial-of-service attacks. *IEEE Systems Journal*. 2022; 17(2): 3246-3257. Available from: https://doi.org/10.1109/JSYST.2022.3214980.

[14] Xu Y, Guo X, Zhang G, Li J, Huo X, Xuan B, et al. A learning control strategy for robot-assisted bathing via impedance sliding mode technique with non-repetitive tasks. *International Journal of Control, Automation and Systems*. 2024; 22(3): 946-962. Available from: https://doi.org/10.1007/s12555-022-0436-6.

[15] Li T, Zakerimanesh A, Ou Y, Badre A, Tavakoli M. Iterative learning for gravity compensation in impedance control. *IEEE/ASME Transactions on Mechatronics*. 2024; 30(1): 119-130. Available from: https://doi.org/10.1109/TMECH.2024.3386407.

[16] Jin X. Formation-based decentralized iterative learning cooperative impedance control for a team of robot manipulators. *IEEE Transactions on Systems, Man, and Cybernetics: Systems*. 2022; 53(2): 872-881. Available from: https://doi.org/10.1109/TSMC.2022.3189661.

[17] Longman RW, Mombaur KD. Investigating the use of iterative learning control and repetitive control to implement periodic gaits. In: *Fast Motions in Biomechanics and Robotics: Optimization and Feedback Control*. Springer; 2006. p.189-218. Available from: https://doi.org/10.1007/978-3-540-36119-0_9.

[18] Guth M, Seel T, Raisch J. Iterative learning control with variable pass length applied to trajectory tracking on a crane with output constraints. In: *52nd IEEE conference on decision and control*. IEEE; 2013. p.6676-6681. Available from: http://dx.doi.org/10.1109/CDC.2013.6760946.

[19] Seel T, Laidig D, Valtin M, Werner C, Raisch J, Schauer T. Feedback control of foot eversion in the adaptive peroneal stimulator. In: *22nd Mediterranean Conference on Control and Automation*. IEEE; 2014. p.1482-1487. Available from: https://doi.org/10.1109/MED.2014.6961585.

[20] Li X, Xu JX, Huang D. An iterative learning control approach for linear systems with randomly varying trial lengths. *IEEE Transactions on Automatic Control*. 2013; 59(7): 1954-1960. Available from: https://doi.org/10.1109/TAC.2013.2294827.

[21] Li X, Xu JX, Huang D. Iterative learning control for nonlinear dynamic systems with randomly varying trial lengths. *International Journal of Adaptive Control and Signal Processing*. 2015; 29(11): 1341-1353. Available from: https://doi.org/10.1002/acs.2543.

[22] Li XF, Xu JX. Lifted system framework for learning control with different trial lengths. *International Journal of Automation and Computing*. 2015; 12: 273-280. Available from: https://doi.org/10.1007/s11633-015-0882-1.

[23] Shen D, Zhang W, Wang Y, Chien CJ. On almost sure and mean square convergence of P-type ILC under randomly varying iteration lengths. *Automatica*. 2016; 63: 359-365. Available from: https://doi.org/10.1016/j.automatica.2015.10.050.

[24] Shen D, Zhang W, Xu JX. Iterative learning control for discrete nonlinear systems with randomly iteration varying lengths. *Systems & Control Letters*. 2016; 96: 81-87. Available from: https://doi.org/10.1016/j.sysconle.2016.07.004.

[25] Shi J, Xu J, Sun J, Yang Y. Iterative learning control for time-varying systems subject to variable pass lengths: Application to robot manipulators. *IEEE Transactions on Industrial Electronics*. 2019; 67(10): 8629-8637. Available from: https://doi.org/10.1109/TIE.2019.2947838.

[26] Ding Y, Jia H, Wei Y, Xu Q, Wan K. An adaptive learning control for MIMO nonlinear system with nonuniform trial lengths and invertible control gain matrix. *Electronics*. 2024; 13(15): 2896. Available from: https://doi.org/10.3390/electronics13152896.

[27] Kong Y, Li XD, Li X. Iterative learning control approach for linear discrete time-varying systems with different initial time points. *Journal of the Franklin Institute*. 2024; 361(6): 106702. Available from: https://doi.org/10.1016/j.jfranklin.2024.106702.

[28] Qiu W, Wang J, Shen D. Iterative learning based convergence analysis for nonlinear impulsive differential inclusion systems with randomly varying trial lengths. *International Journal of Adaptive Control and Signal Processing*. 2024; 38(6): 2056-2073. Available from: http://dx.doi.org/10.1002/acs.3791.

[29] Bondy JA, Murty USR. *Graph Theory with Applications. Vol. 290*. London: Macmillan; 1976.

[30] Demmel JW. *Applied Numerical Linear Algebra*. Philadelphia: SIAM; 1997.

[31] Xu Y, Kanade T. *Space Robotics: Dynamics and Control. Vol. 188*. New York: Springer Science & Business Media; 1992.

[32] Li J, Li J. Adaptive iterative learning control for coordination of second-order multi-agent systems. *International Journal of Robust and Nonlinear Control*. 2014; 24(18): 3282-3299. Available from: https://doi.org/10.1002/rnc.3055.